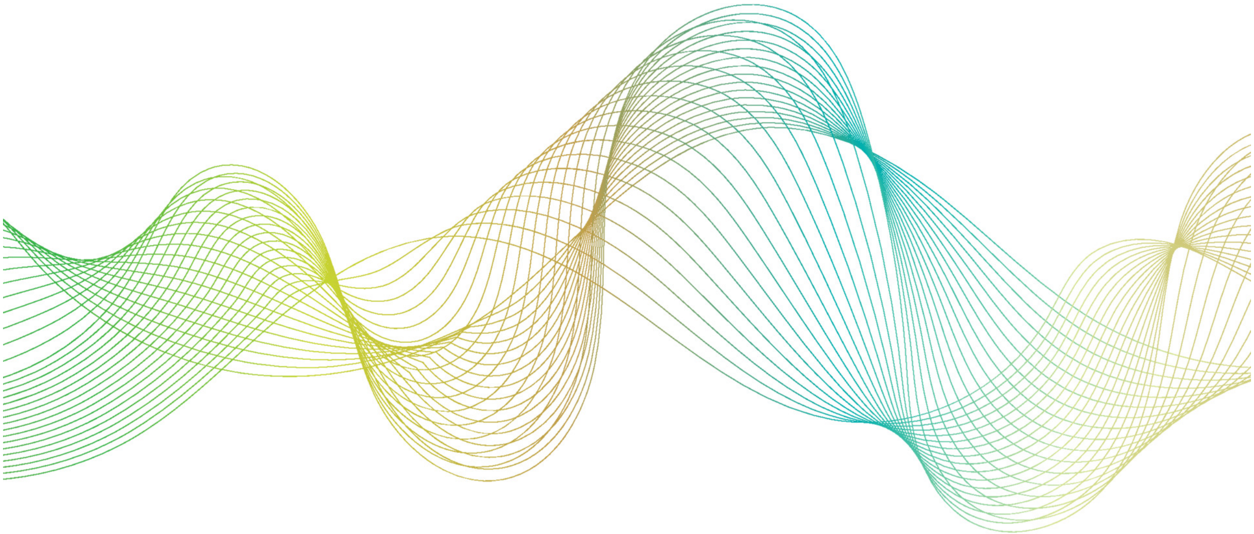

Transmission loss analysis for boat propulsion unit noise shield

Master's thesis in Applied Mechanics

Constanza Montserrat Cruz Sánchez

DEPARTMENT OF MECHANICS AND MARITIME SCIENCES

CHALMERS UNIVERSITY OF TECHNOLOGY
Gothenburg, Sweden 2023
www.chalmers.se

Master's thesis 2023

Transmission loss analysis for boat propulsion unit noise shield

CONSTANZA MONTSERRAT CRUZ SÁNCHEZ

CHALMERS
UNIVERSITY OF TECHNOLOGY

Department of Mechanics and Maritime Sciences
Division of Dynamics
Chalmers University of Technology
Gothenburg, Sweden 2023

Transmission loss analysis for boat propulsion unit noise shield
CONSTANZA CRUZ

Supervisor: Samuel Brauer, NVH engineer, Volvo Penta
Examiner: Håkan Johansson, Professor at Mechanics and Maritime Sciences, Division of Dynamics, Chalmers University of Technology

Master's Thesis 2023
Department of Mechanics and Maritime Sciences
Division of Dynamics
Chalmers University of Technology
SE-412 96 Gothenburg
Telephone +46 31 772 1000

Cover: Abstract Sound Wave Line Background [21].

Printed by Chalmers Reproservice
Gothenburg, Sweden 2023

Abstract

The transition from a diesel engine to an electric engine represents a significant step towards achieving greater sustainability in maritime vessels. However, this conversion can expose tonal noise from the Integrated Propulsion System (IPS) component of a boat propulsion system. Therefore, the main objective of this thesis project is to develop a methodology for assessing sound transmission loss (TL) in components that incorporate absorbent materials as passive noise control measures.

The TL model was constructed using Actran software. The model consisted of a two-layered system composed by wood and foam in combination with a monopole source. Simulations were conducted in a semi-anechoic chamber setup. Two mathematical models, namely the Johnson-Champoux-Allard (JCA) model and the Miki model, were employed to study sound propagation in porous media and evaluate their impact on defining acoustic parameters. In order to determine the flow resistivity of any material when the acoustic properties are unknown, sound absorption and impedance theories were employed within an impedance tube model.

The results demonstrated that accurately defining the complete acoustic parameters in the JCA model is crucial for obtaining reliable results. Furthermore, for accurate prediction of flow resistivity using either sound absorption or impedance values as inputs, impedance measurements must be performed utilizing the Miki model.

The TL results exhibited a good correlation between the physical measurements and the simulations conducted in Actran, using both the Miki Model and JCA model. However, it should be noted that since the Miki model has only one material parameter, it is more sensitive to changes in flow resistivity compared to the JCA model. Consequently, variations in flow resistivity can have a substantial impact on the results and must be carefully considered in the analysis and in the design process.

Keywords: Miki model, JCA model, impedance tube, sound absorption, transmission loss, sound power level.

Acknowledgements

I would like to express my gratitude to Samuel Brauer from the CAE team at Volvo Penta for his unwavering patience and invaluable support throughout this thesis project. I am truly grateful for the knowledge and guidance shared by Stig Kleiven and Jonas Törnqvist, allowing me to learn from their expertise.

I would like to express my sincere gratitude to my examiner, Håkan Johansson, for his guidance, support, and kindness throughout this thesis project. His valuable insights were essential in shaping the direction and quality of my work.

I would also like to extend my thanks to the entire CAE team at Volvo Penta for warmly welcoming me into their work routines and making me feel like a valued member of the group. Your kindness and camaraderie have been greatly appreciated.

Lastly, I am deeply grateful to my family and friends whose support has been my pillar of strength throughout this challenging journey. Your encouragement and belief in me have meant the world.

Thank you all for being a part of my journey and for your invaluable contributions.

Constanza Cruz, Gothenburg, June 2023

List of Acronyms

Below is the list of acronyms that have been used throughout this thesis listed in alphabetical order:

FFT	Fast Fourier transformation
FR	Flow resistivity
JCA	Johnson-Champoux-Allard model
NS	Noise reduction
RMS	Root mean square
SWL	Sound power level
SPL	Sound pressure level
TFM	Transfer function matrix
TL	Transmission loss

Nomenclature

Below is the nomenclature of parameters that have been used throughout this thesis. A dimensionless parameter is stated as [-].

Parameters

ρ_0	Air density [kg/m^3]
A	Amplitude [m]
ω	Angular frequency [rad/s]
α_M	Attenuation constant in Miki model [Neper/m]
W	Averaged sound power [W]
Z_0	Characteristic impedance [Pa s/m^3]
Z_c	Characteristic impedance in Miki model [Pa s/m^3]
ρ	Density [kg/m^3]
K_{eff}	Dynamic bulk modulus [Pa]
ρ_{eff}	Dynamic mass density [kg/m^3]
η	Dynamic viscosity [Pa s]
P_0	Fluid equilibrium pressure [Pa]
σ	Flow resistivity [N s/m^4]
f	Frequency [Hz]
X_M	Imaginary component of characteristic impedance in Miki model. [Pa s/m^3]
P_i	Incident pressure [Pa]
W_i	Incident sound power [W]
ν_0	Kinematic viscosity [Pa s]
T	Period [s]
β_M	Phase constant in Miki Model [rad/m]
ϕ	Phase shift [rad]

ν	Poisson's ratio [-]
Φ_B	Porosity in Biot's model [-]
Φ_{JCA}	Porosity in JCA model [-]
N_p	Prandtl's number of air [-]
p	Pressure [Pa]
γ	Propagation constant [-]
R_M	Real component of characteristic impedance in Miki model. [Pa s/m^3]
P_r	Reflected pressure [Pa]
R	Reflection coefficient [-]
α	Sound absorption [-]
c_0	Speed of sound in air [m/s]
ζ	Specific impedance [-]
c	Speed of sound [m/s]
S_{ij}	Stress tensor for air [Pa]
Z	Surface impedance [Pa s/m^3]
Λ'	Thermal length [m]
d	Thickness [m]
t	Time [s]
α_∞	Tortuosity [-]
τ	Transmission coefficient [-]
P_t	Transmitted pressure [Pa]
W_t	Transmitted sound power [W]
v	Velocity [m/s]
Λ	Viscous length [m]
λ	Wavelength [m]
k_c	wavenumber [1/m]
E	Young modulus [Pa]

Contents

List of Figures

List of Tables

1

Introduction

1.1 Motivation

Sound is an integral part of human activities, with both noise and sound sharing the same physical properties. However, noise is considered an unwanted sound. In daily life, noise can be categorized into two types: ***occupational noise***, which is work-related, and ***environmental noise***, which encompasses all other sources of noise [22]. Although the adverse effects of high noise levels on health have long been recognized, it was not until recent years that companies and governments made significant efforts to prevent occupational noise exposure and establish noise level limits.

Noise pollution in the marine context not only affects human lives but also interferes with flora and fauna, particularly marine mammals [14]. The expanding presence of commercial shipping has necessitated the construction of high-speed and high-capacity ships, thereby causing elevated ambient noise levels in the marine ecosystem. As a result, significant efforts are being dedicated to the analysis of transmission loss in engine rooms and propulsion systems of marine vessels [20].

This thesis project focuses on studying the Volvo Penta hybrid IPS propulsion system as a case of study. The IPS system has a clutch, which provides the driver with the flexibility to choose between the electric engine and a parallel combination of the diesel engine and electric engine for propulsion purposes. However, a challenge arises when opting for the electric-only mode, as tonal noise from the IPS becomes exposed, which was previously masked by the noise generated by the diesel engine.

To address the issue of exposed noise, a potential solution is derived from the passive noise control approach, involving the implementation of a shield as a barrier to minimize noise propagation. In order to measure the effectiveness of this shielding solution, a transmission loss analysis will be conducted. Transmission loss values quantify the shield's ability to effectively block or reduce the propagation of noise energy through the shield, thereby creating a quieter environment on board the vessel. In fig. 1.1 the hybrid IPS system is shown.

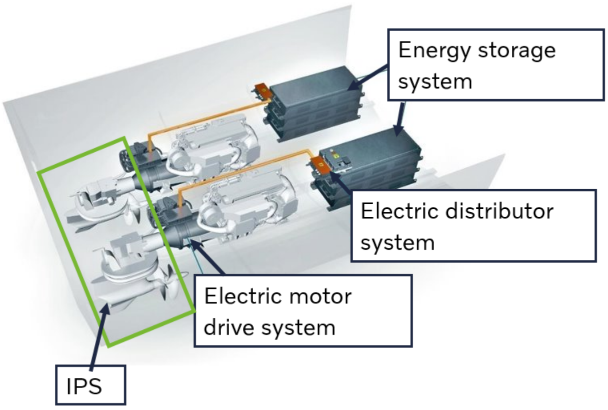

Figure 1.1: Hybrid system IPS [8].

1.2 Objective

This thesis project seeks to develop a methodology to perform air borne noise simulations with the software Actran of a driveline which include a noise shield or noise absorption material having a good correlation with respect to physical measurements.
The specific objective of this project is to:

Perform a transmission loss study using the software Actran to simulate airborne noise propagation through a noise shield and compare the simulation results with physical measurements to evaluate the effectiveness of the simulation.

1.2.1 Research questions

In the context of noise shielding for an IPS, this thesis project addresses the following research questions:

- How does the sound parameters affect the sound absorption and transmission loss?
- How does the number of elements per wavelength impact in the final results?
- How accurate are the simulations in Actran compared to the physical results?

1.3 Approach

In order to accurately predict transmission loss (TL) for any component incorporating a noise shield, it is crucial to compare the ratio of transmitted and incident sound power. Therefore, a model will be done in Actran, which facilitates the transformation of sound pressure into sound power to obtain these values. The frequency range for TL analysis will be (800 - 4000 Hz), damping will be neglected.

The TL analysis in Actran employs an acoustic near and far field, which automatically calculates the averaged radiated power. Additionally, if desired, microphones can be strategically placed at specific locations. A spherical sound source with a constant amplitude in three dimensions will serve as the input force. To simulate the semi-anechoic chamber where the physical noise shield will be tested, Actran allows the creation of a semi-free field condition, which accounts for sound reflection on the floor.

The noise shield is a layered system composed by a porous material and wood. In order to simulate sound propagation in porous media, two sound transmission models will be employed in a Kundt's tube model in Actran. Accurate characterization of the porous material is crucial as noise reduction occurs through the conversion of acoustic energy into heat during interaction with the porous media. Having characterized the porous material enables the correct simulation of sound waves interacting with the porous material and therefore, the calculation of acoustic power and transmission loss. However, material data is not always available. To address this, an in-situ impedance measurement can be used to approximate flow resistivity and define the porous material within the Kundt's tube in Actran.

Finally, in order to establish correlation between simulation and reality, physical measurements will be performed in a semi-anechoic chamber using standard ISO 3744 as a guideline. Dewesoft will be used to record the acoustic pressure and eventually, the Fast Fourier transformation to the frequency domain.

2

Theory

2.1 Literature review

There are several studies for sound absorption and impedance measurements using an impedance tube, also known as *Kundt's tube*, with porous materials. In these cases, the incident waves are standing waves[1] propagating in the axis direction of the tube. Typically, impedance tube tests adhere to the ISO 10534-2 or ASTM E 1050 standards which employ the *transfer function method* to calculate pressure fluctuations caused by the presence of the material being examined at the bottom of the tube. Additionally, impedance tube can also be used to calculate wavelength, speed, transmission loss of a sound wave and more advanced measurements such as macroscopic parameters governing viscous dissipation in porous media [10],[11].

The impedance tube method is not the only one that exists for determining these acoustic parameters. The *room method* has been vastly studied for measuring sound absorption and ISO 354 [13] is the standard that describes and manages this method. Nevertheless, the *room method* requires a reverberation chamber which not every laboratory has.

On the other hand, Caballol et al. [12] conducted a study focusing on transmission loss measurements for rigid building materials. This research is particularly significant because most of the sound absorption measurements in Kundt's tube primarily involve "limp" materials, such as foams, soft rubber, or fibers. The study aims to compare the transmission loss results obtained using Kundt's tube with those obtained through the *two rooms method* described and standardized by ISO 10140 [**??**]. It is worth noting that the impedance tube typically requires the use of two tubes for transmission loss studies. The sample is placed between these tubes, and four microphones are utilized to calculate the pressure, subsequently transforming it into radiated and incident power.

The results for the Caballo et al. project [12] highlighted two main issues: firstly, a substantial disparity in the transmission loss values compared to the *two rooms method*; and secondly, a significant variability in the data, making it unreliable for precise measurement. Consequently, the proposed method was rejected. It is important to note that the results of these two methods were expected to differ due to the distinctive nature of incident waves involved in each approach. In the impedance tube, the incident wave is perpendicular to the sample under testing. Conversely, in the *two rooms method*, the incident wave arrives from random directions as the test is conducted in a reverberation chamber, which generates a diffuse sound field.

[1] Superposition of two waves with the same amplitude and frequency but opposite direction, usually achieved by using a travelling wave and its reflection.

2.2 Airborne sound propagation

The term sound refers to a mechanical wave propagating through a medium, such as air, water, or solids. These vibrations create sound waves that travel through the medium until they reach a listener's ears, where they are interpreted as sound. The sound that we hear consists of fluctuations in the atmospheric air pressure.

In the study of noise it is important to review the concept of waves since noise is modelled as airborne sound propagation. The general wave equation is shown below in equation 2.1. The wave equation models the pressure fluctuation as a function of time and space [1]. In fig. 2.1 a shift in space at a fixed time t is shown, followed by a time wave measured at an arbitrary x. Figure 2.2 shows the oscillatory pattern characteristic of longitudinal waves[2] responsible of creating variation in the air pressure. Compression depicts a region where the particles of the medium are closely packed together, resulting in a higher density of particles. Conversely, rarefaction represents an area where the particles within the medium are dispersed, resulting in a reduced particle density.

$$\frac{\partial^2}{\partial x^2} p(x,t) = \frac{1}{c^2} \frac{\partial^2}{\partial t^2} p(x,t) \tag{2.1}$$

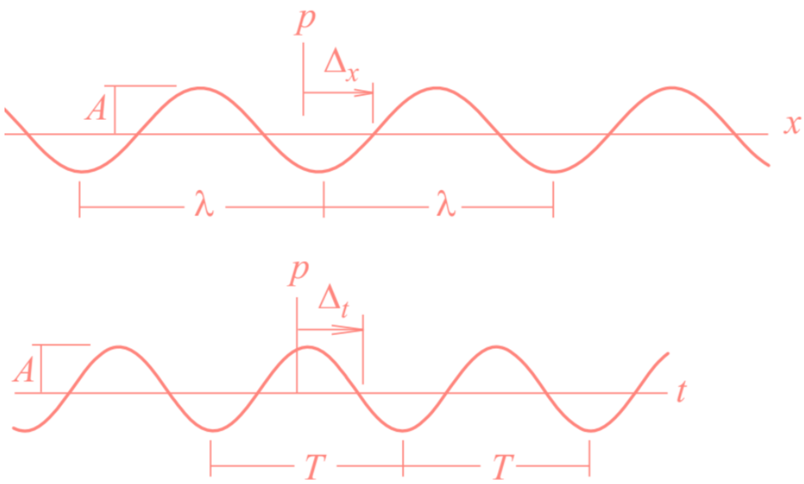

Figure 2.1: Harmonic wave [23] .

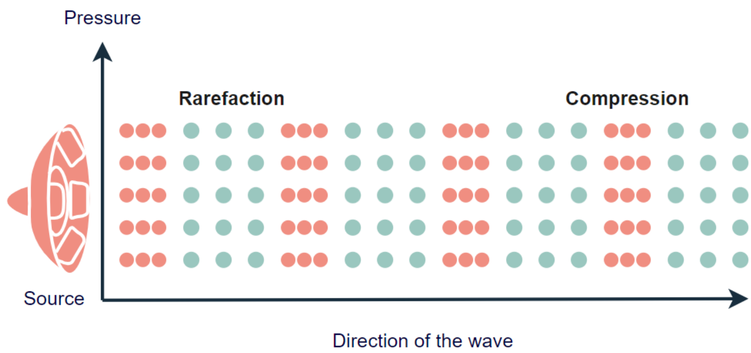

Figure 2.2: Rarefaction and compression for a longitudinal wave.

[2]Longitudinal wave: a wave with a parallel vibration to the propagation's direction.

Sound and vibration problems are often described using harmonic time-dependent functions. The following characteristics are important in defining the pressure according to time and space, see also fig. 2.1.

- Wavelength (λ) represents the spatial shift in position, denoted as x, required to produce a $2\,\pi$ phase alteration while keeping time (t) constant.
- Period (T), is the time needed for the phase of the signal to undergo a $2\,\pi$ alteration.
- Amplitude (A) refers to the maximum absolute value of the wave.
- Angular frequency (ω) characterizes how the phase changes with respect to time.
- Wavenumber (k) measures how many wave cycles exist in one unit of spatial distance.
- Frequency (f) measures the number of complete wave cycles that occur in one unit of time, it is typically measured in Hertz (Hz).
- Speed of sound (c) rate at which sound waves travel through a medium such as air, water or solids.

The following equations relate the previous harmonic waves characteristics.

$$f = 1/T \qquad f = c/\lambda \qquad \omega = 2\,\pi f \qquad \omega = \pm k\, c \tag{2.2}$$

Harmonic sound waves can be modeled using trigonometric functions or Euler's formula as:

$$p(x,t) = A\,\cos(\omega t \mp kx + \phi) \tag{2.3}$$

$$p(x,t) = \mathrm{Re}\left\{A\, e^{i(\omega t \mp kx + \phi)}\right\} \tag{2.4}$$

$$\phi = \tan^{-1}\left(\frac{A\,\cos(\omega\, t)}{B\,\sin(\omega\, t)}\right) \tag{2.5}$$

Where ϕ represents a phase shift in both equations [1]. Equations 2.3 and 2.4 depict the pressure variation in both time and space. However, when considering the complex number representation without isolating the real part (eq. 2.4), it becomes a useful tool for quantifying phase changes within the wave. As a result, the pressure variation can be mathematically expressed as a complex number, although in practical terms, only the real part holds physical significance in the real-world context.

It can be proved that eqs. 2.3 and 2.4 satisfy the general wave equation 2.1. Assuming $p(x,t)$ is described as eq. 2.3, inserted to the left and right hand side of the general wave equation provides the relation between wavenumber and angular frequency stated in eq. 2.2. One solution for the general wave equation (2.1) is presented below.

1. The right hand side of eq. 2.1:

$$\frac{\partial^2 p(x,t)}{\partial x^2} = -A\,\sin(\omega t \mp kx + \phi)\, k^2 \tag{2.6}$$

2. The left hand side of eq: 2.1.

$$\frac{\partial^2 p(x,t)}{\partial t^2} = -A\,\sin(\omega t \mp kx + \phi)\,\omega^2 \tag{2.7}$$

3. Eq. 2.6 and 2.7 into 2.1

$$-A\,\sin(\omega t \mp kx + \phi)\,k^2 = -A\,\sin(\omega t \mp kx + \phi)\,\omega^2\left(\frac{1}{c^2}\right) \tag{2.8}$$

$$k^2 = \frac{\omega^2}{c^2} \tag{2.9}$$

2.2.1 Sound impedance

Acoustic impedance also called *surface impedance* (Z), quantifies the degree of resistance or opposition encountered by a material or medium when sound waves propagate through it. Originally rooted in electronics, impedance analysis extends to acoustics; impedance relates pressure and velocity, both of which may be expressed as complex numbers. Within this context, the real component of acoustic impedance characterizes energy dissipation during wave-boundary interactions, typically resulting from friction and other dissipative processes, while the imaginary component accounts for phase shifts in these interactions.

Regarding impedance as a surface boundary, it is defined as the pressure at a fixed point in a non-moving flat surface and the particle's velocity normal to the surface ($\hat{n}$). For a longitudinal wave, the impedance is a constant denominated *characteristic impedance* denoted in this report as Z_0. Finally a dimensionless ratio which can be useful handling mathematical equations is denoted as *specific impedance* (ζ).

$$Z = \frac{p(x,t)}{v(x,t)} \tag{2.10}$$

$$Z_0 = \rho\,c \tag{2.11}$$

$$\zeta = Z/Z_0 \tag{2.12}$$

where:

$$v(x,t) = \frac{\partial^2}{\partial x \partial t}\left(\frac{A}{\rho\,\omega^2}\cos\left(\omega\,t - k\,x + \phi\right)\right) \tag{2.13}$$

2.2.2 The complex representation

Dissipative processes such as viscosity and heat conduction significantly impact the macroscopic description of sound propagation, leading to the necessity of representing density (ρ) and bulk modulus (K) of the media as complex quantities. Consequently, key parameters such as velocity (c), wavenumber (k), and impedance (Z) assume complex values in the context of these processes [26].

$$k = \mathrm{Re}(k) + \mathrm{j}\,\mathrm{Im}(k) \tag{2.14}$$

$$Z = \mathrm{Re}(Z) + \mathrm{j}\,\mathrm{Im}(Z) \tag{2.15}$$

It is important to remember that many of the physical effects in sound propagation depend on the wave length. Therefore, many of the parameters used to describe sound propagation are treated and analyzed as functions of frequency (ω), and most of the analysis is carried out in frequency domain using the complex representation.

2.3 Sound propagation in porous media

Biot's model describes sound wave propagation in a porous media saturated with a fluid [7]. The model considers a porous medium composed by two phases; a ***fluid phase*** where the sound wave travels through and a ***solid phase*** which represents the skeleton of the material and transmits the pressure load to the filled pores. Both phases are assumed elastic in Biot's model.

Biot's mode define three types of sound waves; one pressure wave in the *fluid phase,* and one pressure and shear wave *in the solid phase* [6]. In Biot's theory the frame and air move simultaneously thus, deformations of the system related with the wave propagation are supposed to be similar as in an elastic solid.

$$S_{ij} = -\Phi_B \, p \, \delta_{ij} \tag{2.16}$$

where:

$$\begin{aligned}
\Phi_B &= \text{Porosity} \\
p &= \text{Pressure} \\
S_{ij} &= \text{Stress tensor for air} \\
\delta_{ij} &= \text{Kronecker delta}
\end{aligned}$$

Building upon the Biot's model, several subsequent models have emerged which consider the solid phase as rigid. Nevertheless, the properties of the fluid also account for the wave propagation in the skeleton. These models are called *fluid models* [6], examples of such are Miki model and the JCA model.

2.3.1 Miki Model

Miki model is a semi-empirical model based on the work from Delany and Bazley, were the only acoustic parameter to be defined is the flow resistivity. Delany and Bazley developed mathematical formulas using empirical data acquired from glass wool and rock wool. Miki subsequently made adjustments to the coefficients and exponents in order to ensure that the resulting expressions maintain the desirable positive-real property for both the real (R_M) and imaginary (X_M) components [18]. According to Delany and Bazely, the acoustical properties of a porous material, are the characteristic impedance (Z_c) and the propagation constant (γ) defined below.

$$Z_c = R_M + jX_M \tag{2.17}$$

$$\gamma = \alpha_M + j\beta_M \tag{2.18}$$

where:

$$R_M = \rho_0\, c_0 \left\{ 1 + a \left(\frac{f}{\sigma} \right)^b \right\} \tag{2.19}$$

$$X_M = -\rho_0\, c_0 \left\{ c \left(\frac{f}{\sigma} \right)^d \right\} \tag{2.20}$$

$$\alpha_M = \frac{\omega}{c_0} \left\{ p \left(\frac{f}{\sigma} \right)^q \right\} \tag{2.21}$$

$$\beta_M = \frac{\omega}{c_0} \left\{ 1 + r \left(\frac{f}{\sigma} \right)^s \right\} \tag{2.22}$$

The term $\left(\frac{f}{\sigma} \right)$ is a coefficient defined as:

$$0.01 < \left(\frac{f}{\sigma} \right) < 1 \tag{2.23}$$

Coeff.	Degree
a = 0.0699	b = -0.632
c = 0.107	d = -0.632
p = 0.160	q = -0.618
r = 0.109	s = -0.618

Table 2.1: Coefficients and degrees for Miki model, material independent.

2.3.2 JCA Model

The Johnson-Champoux-Allard model is a semi-phenomenological model which provides sound absorption values with good agreement respective impedance tube values since it considers viscous-inertial and dissipative effects [24],[25]. The impedance equation for this model is described below, followed by a brief description of the 5 parameters.

$$Z_c(\omega) = \sqrt{\rho_{eff}\, K_{eff}} \tag{2.24}$$

$$k_c = \omega \sqrt{\frac{\rho_{eff}}{K_{eff})}} \tag{2.25}$$

where:

$$\rho_{eff} = \frac{\alpha_\infty \rho_0}{\Phi_{JCA}} \sqrt{1 + j \frac{4\, \alpha_\infty \eta\, \rho_0\, \omega^2}{\Phi_{JCA}^2 \Lambda^2 \sigma}} \tag{2.26}$$

$$K_{eff} = \frac{\gamma\, P_0 / \Phi_{JCA}}{\gamma - (\gamma - 1) \left(1 - j \frac{8\eta}{\Lambda'^2\, \omega\, \rho_0\, N_p} \sqrt{1 + j \frac{\Lambda'^2\, N_p\, \rho_0\, \omega}{16\, \eta}} \right)^{-1}} \tag{2.27}$$

- Flow resistivity (σ): ability of the material to oppose flow through it due to its internal visco-inertial effects.
- Porosity (Φ_{JCA}): ratio between the volume of the fluid and the total volume of the porous material.
- Tortuosity (α_∞): measure of the intricate paths that sound waves must travel through the porous material being 1 a straight path.
- Viscous length (Λ): parameter that describes viscous effects in porous materials.
- Thermal length (Λ'): parameter that describes thermal effects in porous materials.

Figure 2.3: JCA acoustic parameters

2.3.3 Sound absorption

Sound absorption (α) is a dimensionless parameter which defines the amount of acoustic energy that is removed from an acoustic wave as the wave travels through a wall or material. Sound absorption is frequency and thickness dependent, and its values are normally between ($0 < \alpha < 1$). A sound absorption value equal to 0 means that 100% of the wave was bounced back without loses.
Sound absorption is defined as:

$$\alpha = 1 - |R|^2 \tag{2.28}$$

where:

R = Reflection coefficient

Z_0 = Air impedance, normally around 415 $\left[\frac{\mathrm{kg}}{\mathrm{m}^2\,\mathrm{s}}\right]$, (pressure and temperature dependent).

$$Z_0 = \rho\, c \left[\frac{\mathrm{kg}}{\mathrm{m}^2\,\mathrm{s}}\right] \tag{2.29}$$

$$R = \frac{\frac{p}{v} - Z_0}{\frac{p}{v} + Z_0} \tag{2.30}$$

2.3.4 Sound pressure and sound power

Sound power (SWL) and sound pressure (SPL) levels are commonly expressed in decibels (dB), but it is important to note that they convey different information. The decibel is a logarithmic scale used to compare two quantities. While both SPL and SWL are denoted in decibels, they represent distinct aspects. SPL characterizes the acoustic field at a specific location in space, SWL represents the total amount of energy radiated by a sound source in all directions.

$$SPL = 10\,\log_{10}\left(\frac{p^2}{P_{ref}^2}\right) \quad [\text{dB}] \tag{2.31}$$

Where P_{ref} is a reference pressure, usually taken as 2×10^{-5} for airborne sound and 2×10^{-6} for underwater sound, p is the (RMS) pressure in Pa.

$$SWL = 10\,\log_{10}\left(\frac{W^2}{W_{ref}^2}\right) \quad [\text{dB}] \tag{2.32}$$

Where W_{ref} is a reference pressure, usually taken as 1×10^{-12}, W is the averaged sound power [2].

2.4 Transmission loss

As mentioned early in this thesis report, a barrier between a sound source and a listener can effectively reduce the noise perception of the listener. The ability of sound to be transmitted trough a barrier is called transmission loss (TL).
TL is calculated as a sound wave transmitted relative to an incident sound wave. In fig. 2.4 it can be seen the classic representation of TL where P_i represents the sound pressure level (SPL) of an incident wave, P_r represents the reflected wave and P_t the transmitted wave. Transmission loss is calculated as:

$$TL = 10\,\log_{10}\left(\frac{1}{\tau}\right) \tag{2.33}$$

where:

$$\tau = \left|\frac{P_t}{P_i}\right|^2 \tag{2.34}$$

The simplest way to define TL and the transmission coefficient (τ) is assuming the wall as a limp mass (no damping, no stiffness). Assuming the wall is at $x = 0$ and a harmonic sound field with frequency given in rad/s, the pressure at the incident side of the wall ($x < 0$) and the pressure at the transmitted side of the wall ($x > 0$) are written in Eqs. 2.35 and 2.36 respectively. As mentioned in Eq. 2.34, the transmission coefficient is the ratio between the transmitted pressure (P_t) and the incident pressure (P_i) [5]:

$$p(x,t) = e^{iwt}\,(P_i\,e^{-ikx} + P_r\,e^{ikx}) \tag{2.35}$$

$$p(x,t) = P_t\,e^{iwt}\,e^{-ikx} \tag{2.36}$$

Defining the transmission coefficient (τ) is critical to calculate the transmission loss. Estimating τ can be done with Newton's equations, however for complex systems such as layered systems or nonlinearities, the transfer function method is used. In this thesis project the transfer method was done by Actran.

As stated in section 2.3.4 SPL and SWL state for different information. Sound pressure, as defined in equation 2.3, is both position and time dependent, whereas SWL is not. Therefore, in the analysis, it is preferable to use SWL due to its independence from specific positions. The TL equation using sound power is defined as:

$$TL = 10 \log_{10} \left(\frac{W_i}{W_t} \right) \tag{2.37}$$

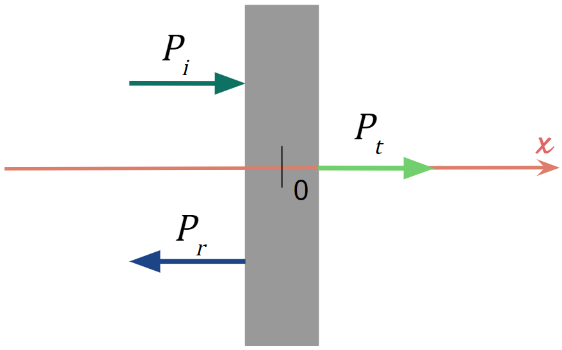

Figure 2.4: Sound wave transmission trough a lumped wall.

2.5 Weighted sound

In section 4.2, SPL and SWL are going to be calculated from in situ measurements following standard ISO 3744. This standard employs A-weighted SPL for calculating SWL. Thus, it's crucial to grasp the distinctions between A, C, and Z-weighted sound. Nonetheless, C-weighted SPL is not employed in this project.

Weighted sound refers to an adjustment in the SPL measurements done by a microphone in order to capture better the human ear sensitivity to sound. This adjustment comes from two main differences between the human ear and a microphone recording. The first one is the fact that human ear has an internal cavity which creates resonance up to 4000Hz, causing a higher perception of sound compared to a microphone diaphragm[3] [3]. The second one is the frequency range human ear can perceive (500Hz - 4kHz) and the fact that a human ear has the human body (torso, head, etc) which changes the perceived sound since it acts as a barrier object. Weighting can not be applied in time-domain, since the weighting is frequency-dependent. There are 3 weighted bands:

- A-weighted : frequency range for human ear noise perception, it covers the full frequency range (20Hz-20kHz). Nevertheless, the human ear is particularly sensitive to sound frequencies between 500 Hz - 4 kHz whilst at lower and higher frequencies the human ear is not very sensitive.
- C-weighted : frequency range focused on low frequencies (it is as well adjusted for human ear sensitivity). This range is flat between 30Hz-8kHz. It is used to measure peak sound levels, impulse noise and occupational noise[4].
- Z-weighted : Flat frequency response without adjustment for the human ear (*Z* for *zero*, not weighted). It is mostly used for determining environmental noise[5].

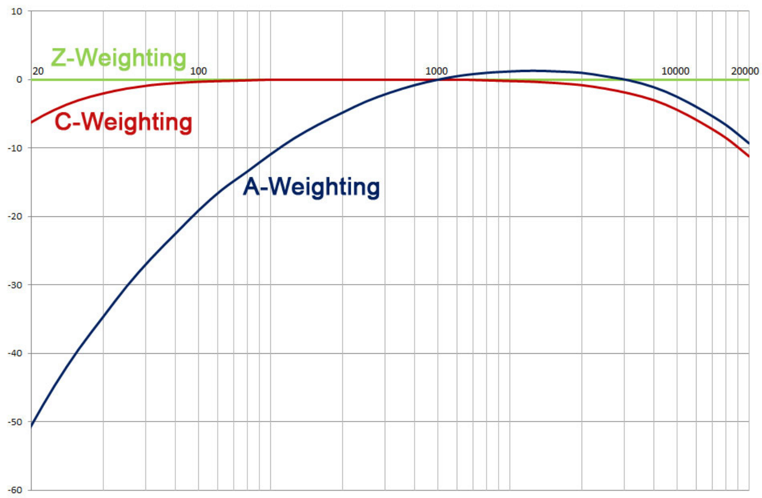

Figure 2.5: A, C and Z frequency weightings for sound.[4]

[3]Acoustic transducer that transforms electric energy into acoustic energy and vice versa.
[4]Noise in workplaces, set as 80 dB for 8 hours labor.
[5]Noise generated from all sources except workplaces.

3

Impedance tube model

3.1 Sound absorption and impedance calculation

As outlined in Section 2.1, an impedance tube proves useful in measuring impedance and sound absorption properties. The objective was to develop a model capable of estimating sound absorption and impedance values for any material, enabling the determination of flow resistivity and characterization of porous materials. To achieve this, a mesh was generated using ANSA, the dimensions for the mesh were obtained from a real Kundt's tube from by Brüel & Kjær, generally, the measurements for Kundt's tubes are divided into two sections due to changes in the frequency range across the tube's diameter. However, for the purpose of this thesis project, only the smaller tube section was utilized[1]. The model configuration is illustrated in fig. 3.1. Several materials were tested with both Miki and JCA model, the material properties are shown in table 3.1. Initially, material AF01 was selected from Actran's material library as it is classified as a polyurethane foam. However, it is worth noting that its thickness was not specified or defined.

- **Finite volume component**: which represents the air in the tube. The properties for the finite volume were $c = 340$ [m/s] and $\rho = 1.225$ [kg/m^3].
- **Rigid porous component**: which represents the foam material. Actran offers different approaches to model the characteristics of a porous material (Miki Model, Delaney Banzey, etc). To represent the JCA model the *Rigid porous* component was used.
- **Velocity boundary condition (BC)**: to excite the system, since it represents a change in the velocity of the medium therefore, it causes the waves to reflect, refract and interfere with each other, creating standing waves which is desired. The velocity BC was specified only in the Z-axis (large of the tube) with a nominal value of 1 Pa $\approx$ 94 dB.

	Unit	MAT 1	MAT 2	AF01
Flow resistivity	$\mathrm{N\,s/m^4}$	25 100	19 600	22 000
Porosity	-	0.95	0.96	0.97
Tortuosity	-	1.26	1.03	1.38
Viscous length	μm	77	66	17
Thermal length	μm	134	178	40
Thickness	m	0.31	0.15	unknown

Table 3.1: Material's acoustic parameters from internal database.

[1]ISO 10534-1 standard provides equations for determining the dimensions of the impedance tube.

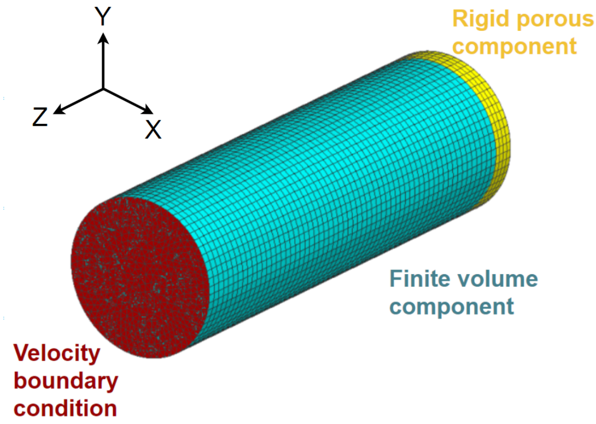

Figure 3.1: Impedance tube Actran model [19].

	Unit	Large tube	Small tube
Diameter	mm	100	30
Length	mm	1050	900
Frequency range	Hz	50 - 1600	500 - 6400

Table 3.2: Kundt's tube dimensions [9].

3.2 Mesh convergence

To assess the mesh convergence of the model, a total of 9 models were created, each with a progressively smaller element size ranging from 30 mm down to 3 mm.

For all the models, the pressure was measured at a specific point, considering the maximum frequency to be analyzed (4000 Hz), the results are shown in fig. 3.2. Actran includes a tool to calculate the minimum element size required to achieve a desired number of elements per wavelength. In this case, the goal was to have at least 8 elements per wavelength for linear mesh order or 6 elements per wavelength for quadratic mesh order. However, this calculation can also be performed manually. Since the wavelength becomes shorter at higher frequencies, it is crucial to ensure that the smallest wavelength has at least 8 elements to meet the desired mesh resolution, for the case $f = 4000$ Hz.

$$\lambda = \frac{c}{f}\,[\mathrm{m}] \tag{3.1}$$

$$\lambda = 0.085\,[\mathrm{m}] \tag{3.2}$$

$$\text{element size} = 0.085/8 \;=\; 0.011\,[\mathrm{m}] \tag{3.3}$$

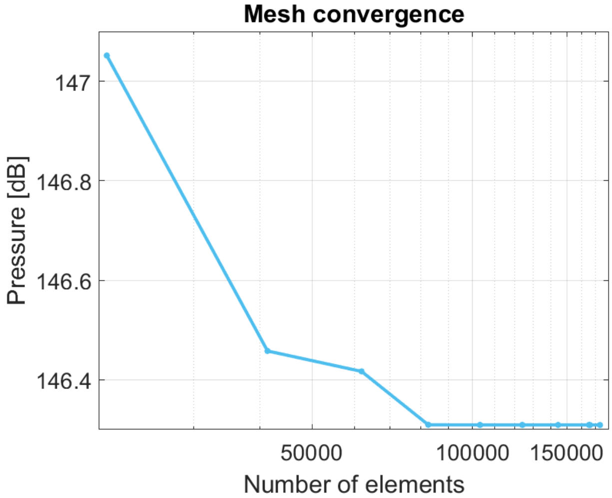

Figure 3.2: Mesh convergence for 4000 Hz

3.3 Impedance tube results

In order to verify the accuracy and therefore the reliability of the model, the calculated sound absorption values were compared with physical measurements. To obtain sound absorption values, pressure and velocity data obtained from Actran simulations were utilized using equations (2.28 - 2.30).

To further assess the model's performance, the Miki and JCA models were defined and analyzed. In fig. 3.3, the sound absorption results are presented for MAT 2, indicating that the JCA model provides more accurate results compared to the Miki model. The Miki model still shows a close approximation to the real measurements. Additionally, fig. 3.3 highlights the significance of the sample thickness in the accuracy of the results. Since the flow resistivity is thickness dependent, it is not accurate to directly compare samples of different thicknesses with respect to those measured in the laboratory not even with the JCA model.

3.3.1 Sound absorption

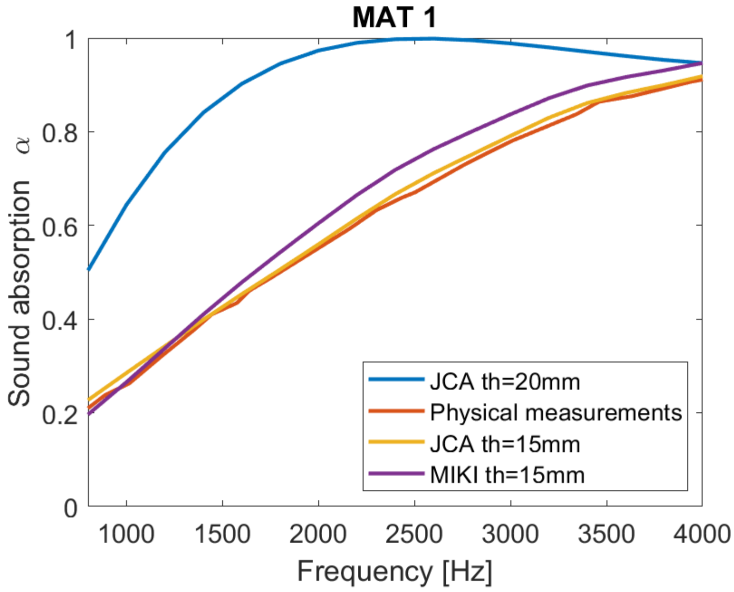

Figure 3.3: Sound absorption for MAT 2, varying thickness and methods. The sample thickness from physical measurements was specified as 15 mm as stated in table 3.1, a change in thickness can significantly impact the behavior of the material.

The project aimed to analyze the influence of parameters in the JCA model, and for this purpose, the five parameters were varied to observe their impact on the material's sound absorption behavior. The results of these variations are presented in fig. 3.4. Each figure in the series represents a single parameter being changed, but it is also possible to combine multiple parameter changes. However, considering the numerous possible combinations, the scope of parameter variations and its results is extensive and its analysis is left out. The crucial observation to make is that the behavior of MAT 1 does indeed change when their acoustic parameters vary, as depicted in fig. 3.4. It is evident that changes in tortuosity, viscous and thermal length can lead to significant alterations in the material's ability to reflect, absorb and refract sound waves.

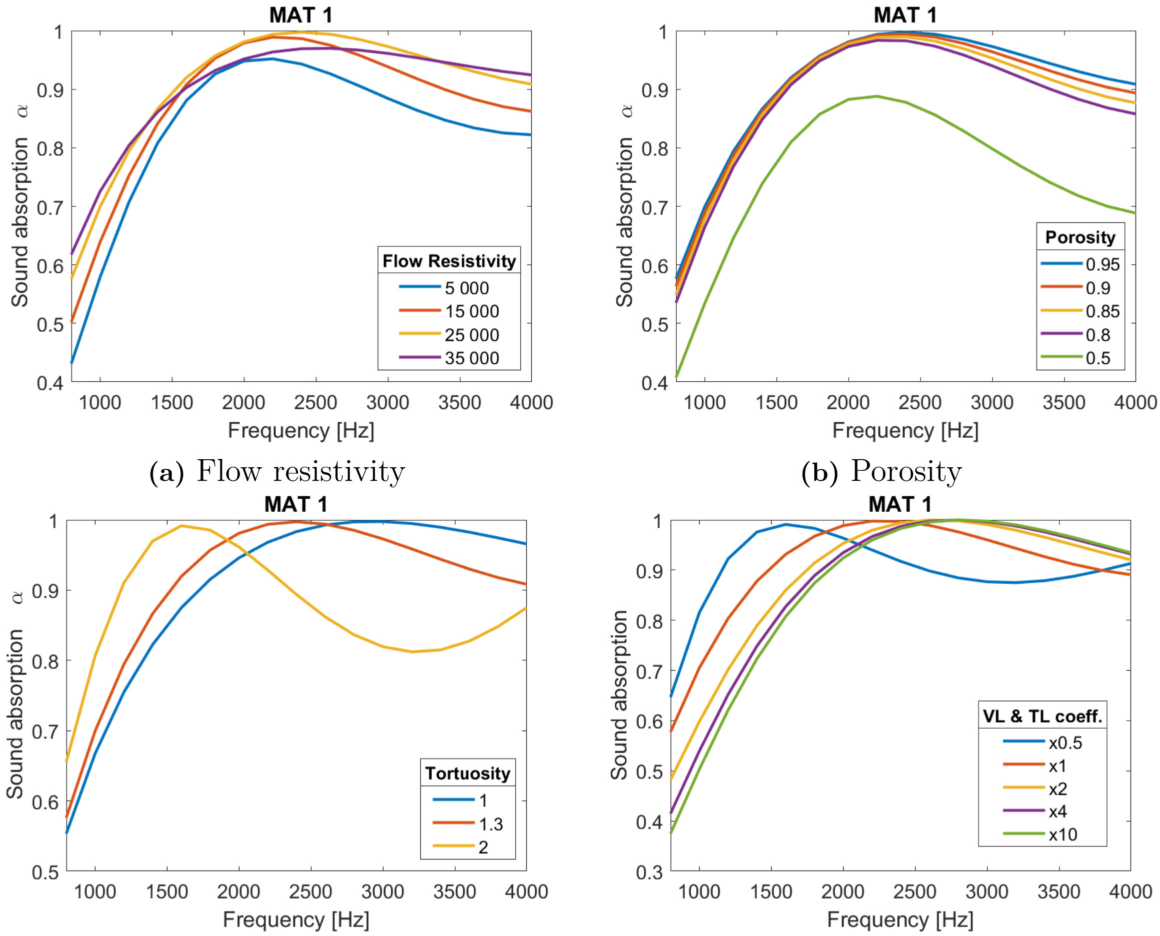

(a) Flow resistivity

(b) Porosity

(c) Tortuosity

(d) Viscous and thermal length[1]

Figure 3.4: Sound absorption variation with respect to changes in material's parameters.

[1]The terms "x0.5", "x1", etc. depict a multiplication factor of the original MAT 1 viscous and thermal length properties.

4

Transmission Loss

4.1 Transmission Loss model

The transmission loss model in Actran was developed based on the dimensions provided in table 4.1. The model consists of various components, which are described below. The Actran model itself is depicted in fig. 4.1 and a transverse view is depicted in fig. 4.2. Initially, since the specific material parameters were unknown and only identified as polyurethane foam, a polyurethane foam from Actran's library was selected for the simulations. However, as it will be discussed in Section 4.4, the obtained results for TL showed a good correlation with this material. In order to enhance the simulation accuracy and reliability, similar materials with known properties and thicknesses were sought from the shared database to perform a more precise simulation with trustworthy data.

- **Spherical source** in the center of the shield and positioned *"on the floor"* ($z = 0$) as the physical arrangement shown in fig. 4.5b, 4.5c. The source input was define as 1 [Pa] equivalent to 94 dB.
- **Finite Volume** which represents the air in the cavity, the properties of the air were $c = 340$ [m/s] and $\rho = 1.225$ [kg/m^3].
- **Porous Rigid** to represent the polyurethane foam. The properties for this component are shown below in table 4.3.
- **Rigid solid** to represent the plywood that covers the shield. The wood from the noise shield was identified as poplar plywood and its elastic properties were defined as $\mathrm{E} = 4$ GPa, $\rho = 515$ kg/m^3 and $\nu = 0.3$ [16].
- **Exterior acoustic** to measure the SPL outside the shield, the exterior acoustic component is defined by a near and a far field. A semi-free field was defined at $z = 0$ to specify the floor as a reflecting material.

	Unit	Dimensions
Length	cm	73
Height	cm	52
Width	cm	64

Table 4.1: Shield dimensions.

	# elements	Max. length [m]	Min. length [m]
Finite Volume	192 000	0.010907	0.010795
Rigid porous	59 988	0.010907	0.01
Rigid Solid	45 512	0.010907	0.0065
Ext. acoustics	545 607	0.035	0.0025

Table 4.2: FE - model mesh specifications.

FA01		
	Unit	Value
Flow resistivity	N s/m	22 000
Porosity	-	0.97
Tortuosity	-	1.38
Viscous length	m	1.7e-5
Thermal length	m	4e-5

Table 4.3: Porous rigid component specifications.

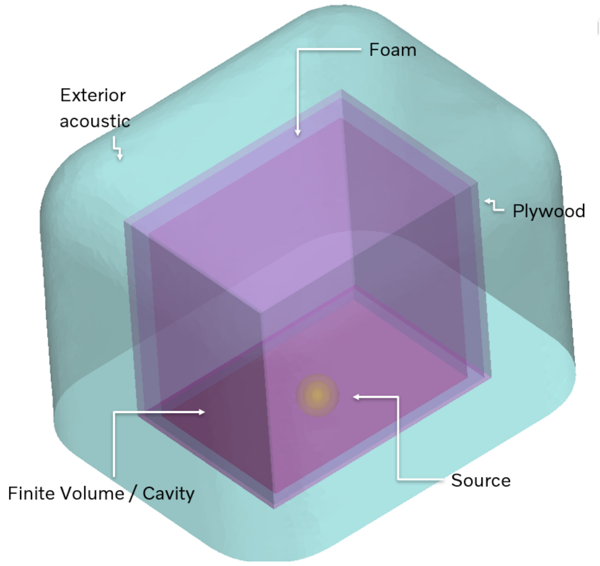

Figure 4.1: Noise shield Actran model.

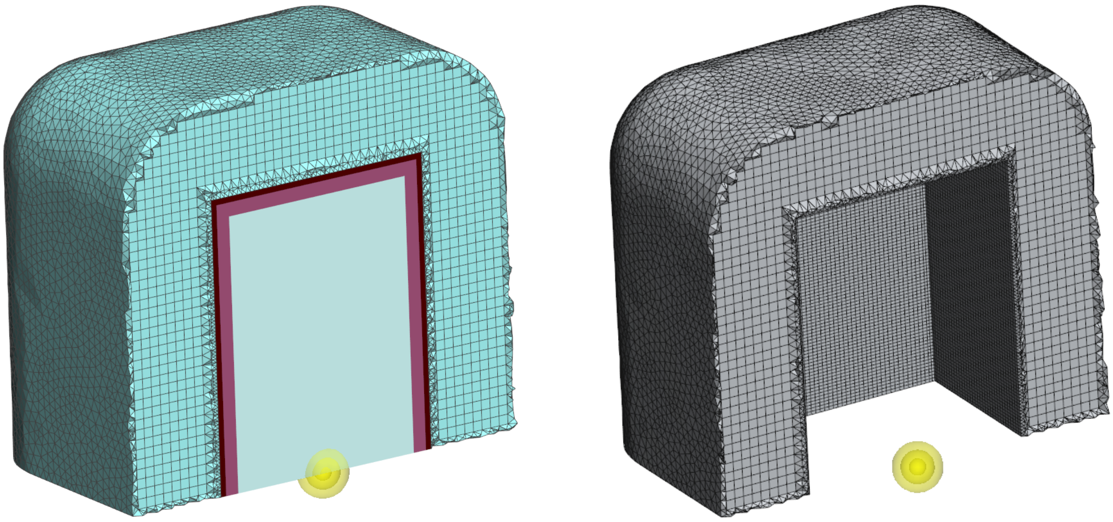

(a) Complete model

(b) Exterior acoustic mesh

Figure 4.2: Actran model transverse detail, figure (a) shows the cavity, foam ,wood and exterior acoustic mesh from inside to outside respectively. Figure (b) shows only the exterior acoustic, defined 0.2 m apart from the shield. The number of elements in the exterior acoustic mesh, provided 4 elements per wave length in the analysis.

4.2 Physical measurements

The noise shield constructed at Volvo Penta is illustrated in fig. 4.3, with the dimensions specified in table 4.1. The shield was built using plywood and polyurethane foam; Nevertheless, the properties of these materials were not known. The measurements were conducted using the equipment outlined in table 4.4. To perform the physical measurements, standard ISO 3744 was employed as a reference. This standard not only served as a guide but also provided the equations for the averaged sound pressure and sound power calculation based on the test environment and specific conditions. These equations are defined below in section 4.3.1.

To conduct the physical measurements, the microphones underwent calibration in Dewesoft. Two microphones were utilized, and a total of four measurements were carried out by switching their positions to cover a constant radius around the source. A velocity source was used as a monopole source, as illustrated in fig. 4.5b. According to the standard requirements, background noise was measured prior to the main measurements. The background noise level had to be at least 10 dB lower than the intended target to ensure reliable measurements. Subsequently, the source was measured without the shield, following the same arrangements as depicted in fig. 4.4. Finally, the source was covered with the shield, fig. 4.5d, and the sound pressure was measured once again.

(a) (b)

Figure 4.3: Noise shield (a) and transverse section detail (b).

Equipment	Model	Purpose
Microphones	TYPE 4189-A-021	Measure SPL
Audio signal generator	MR-PRO/MR2	Wave generator
Volume source	Q-MHF	Omnidirectional source
Power Amplifier	Q-AMP	Amplifier for Q source

Table 4.4: Equipment used in measurements.

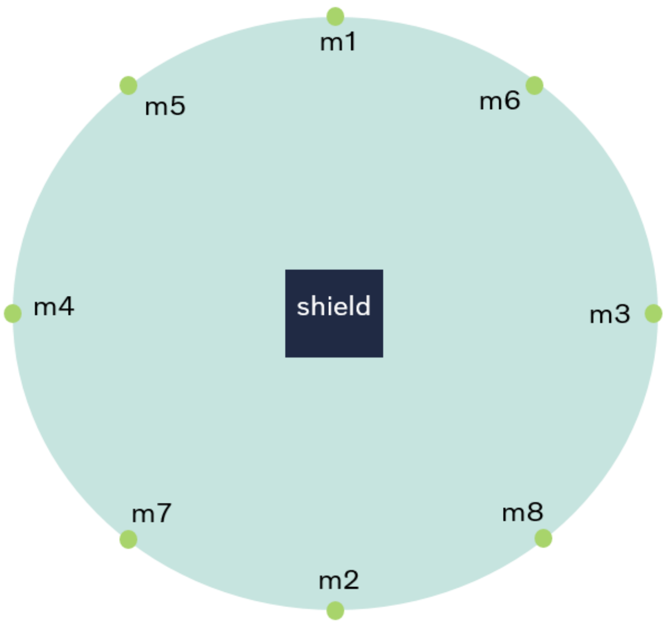

Figure 4.4: Microphone positioning for pressure measurements.

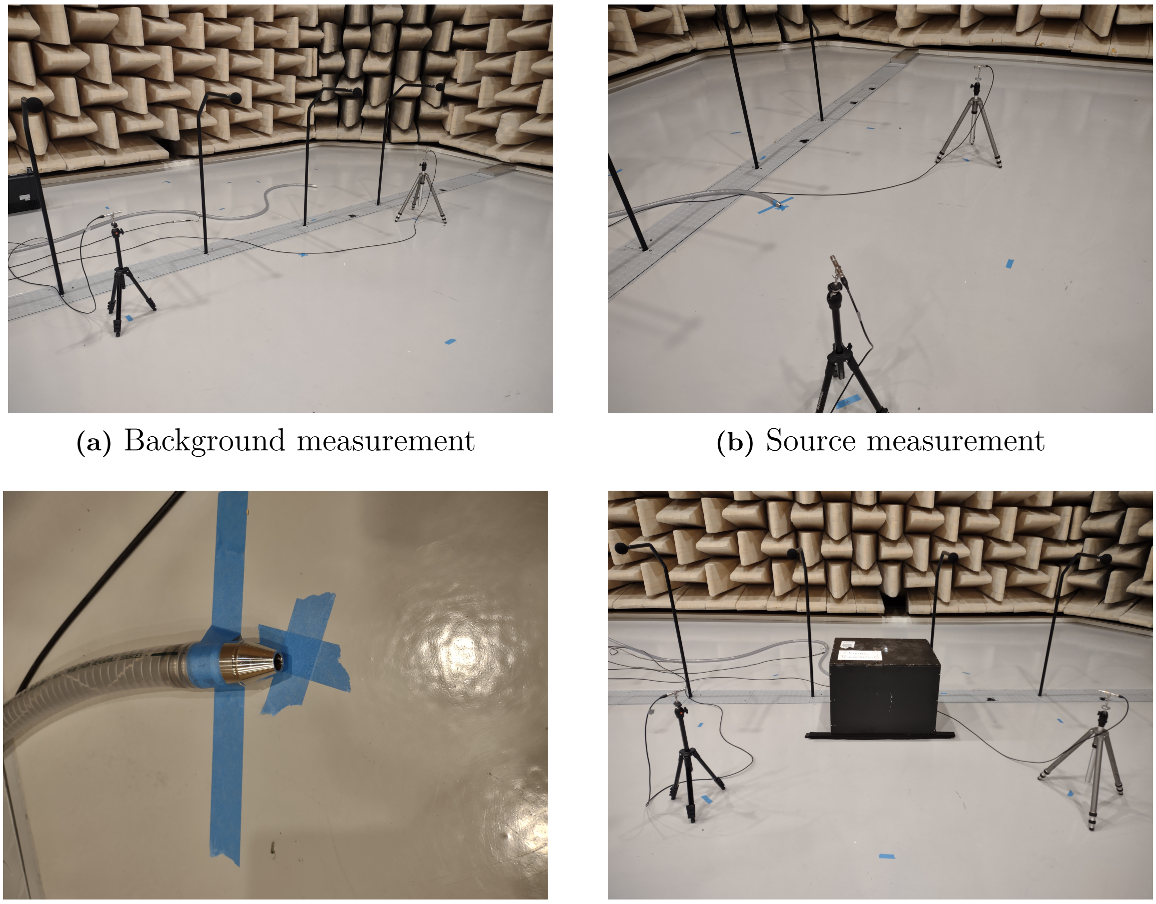

(a) Background measurement

(b) Source measurement

(c) Source nozzle detail

(d) Noise measurement with shield

Figure 4.5: Physical measurements arrangement

4.3 Post-processing with Dewesoft

Time-dependent sound pressure data was obtained from the physical measurements described in section 4.2, which can be challenging to interpret and replicate accurately. To assess these difficulties, most acoustic analyses are conducted in the frequency domain with the assistance of the fast Fourier transform (FFT) method, which was calculated using Dewesoft. This approach allows the determination of desired parameters such as SWL.

The measured sound pressure level was converted into sound power level using equation 4.1. To obtain accurate results, an average of all the measurements was required, this was obtained using equation 4.5. This averaging equation was applied to the source measurements with and without the shield. By comparing these results, a transmission loss analysis was conducted using equation 2.37.

4.3.1 Sound power level calculation

All values are expressed in dB.

$$L_W = \overline{L_p} + 10 \log_{10}\left(\frac{S}{S_0}\right) \tag{4.1}$$

where:

$\overline{L_p} = \overline{L,_{p(\mathrm{ST})}} - K_1$
$S =$ area in $[m^2]$ of the measurement surface
$S_0 = 1\,m^2$

$$K_1 = -10 \log_{10}\left(1 - 10^{-0.1\,\Delta LP}\right) \tag{4.2}$$

$$\tag{4.3}$$

where:

$$\Delta L_p = \overline{L,_{p(\mathrm{ST})}} - \overline{L_{p(\mathrm{B})}} \tag{4.4}$$

in which:

$\overline{L,_{p(\mathrm{ST})}} =$ A-weighted time-averaged SPL in dB
$\overline{L_{p(\mathrm{B})}} =$ A-weighted time-averaged SPL of background noise in dB

4.3.2 Mean-time averaged sound pressure levels

$$\overline{L,_{p(\mathrm{ST})}} = 10 \log_{10}\left[\frac{1}{N_M}\sum_{i=1}^{N_M} 10^{0.1 L,_{pi(\mathrm{ST})}}\right] \tag{4.5}$$

in which:

$L,_{pi(\mathrm{ST})} =$ A-weighted time-averaged SPL at the ith microphone position in dB
$N_M =$ Number of microphones positions

4.4 Transmission loss results

4.4.1 Physical measurements

After the measurements in the anechoic chamber, the calculations for mean-time averaged SPL and SWL were conducted using MATLAB. The values in the frequency domain were obtained with Dewesoft as well as the A-weighted sound. The narrow band results were exported with a frequency step of 50 Hz, while the 1/3 octave band calculations were automatically handled by Dewesoft. In fig 4.6, the results for two different frequency ranges are presented. As stated in the problem limitations, the frequency range of interest was defined as [800 - 4000 Hz], as depicted in In fig 4.6b. Nevertheless, Dewesoft performed an FFT analysis up to 25,000 Hz.

Figure 4.7 illustrates the values for the background noise in relation to the source, as well as the values for the source in relation to the shield. Figure 4.7 depicts the background noise with a Sound Pressure Level (SPL) of 10 dB, while the noise emitted by the source had an approximate SPL of 60 dB. On the other hand, the noise level measured with the shield was found to be 30 dB. Without conducting a reproducibility and repeatability analysis, the measurements of source and background noise without the noise shield was found to exhibit good repeatability. However, when the shield is used there is a higher variance among them, with an average value in a range between 20-30 dB.

Finally, to provide a graphical visualization of the noise levels obtained from the physical measurements, fig. 4.8 displays the averaged SPL for the source, shield, and background sound. This visualization serves to validate the suitability of the study environment. It is important to note that for accurate transmission loss analysis, the measurements of the shield and background noise should be at least 10 dB lower than the source noise level.

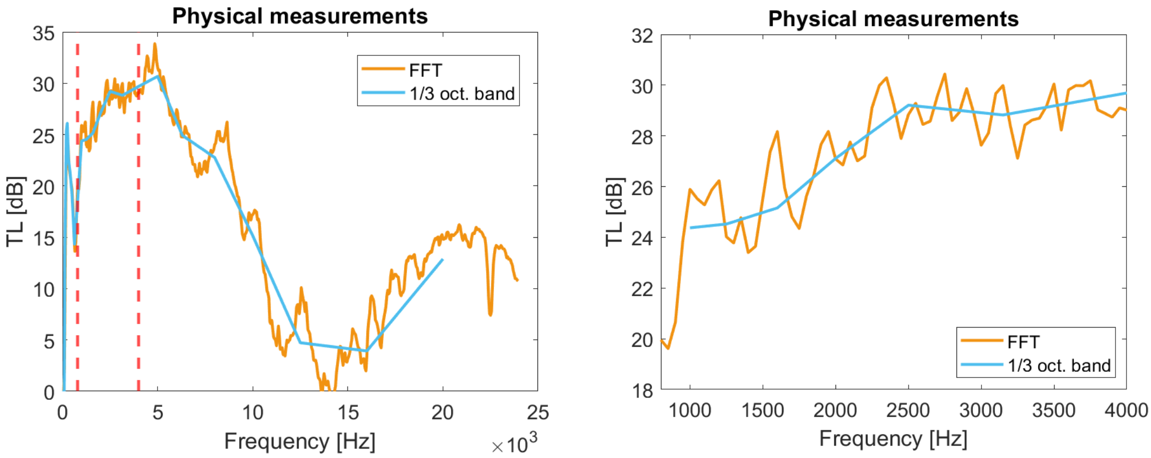

(a) Narrow band

(b) 1/3 octave band

Figure 4.6: Transmission loss results for different frequency bands, fig. 4.6b is a zoom from the narrow band results marked with red-dotted lines in fig. 4.6a.

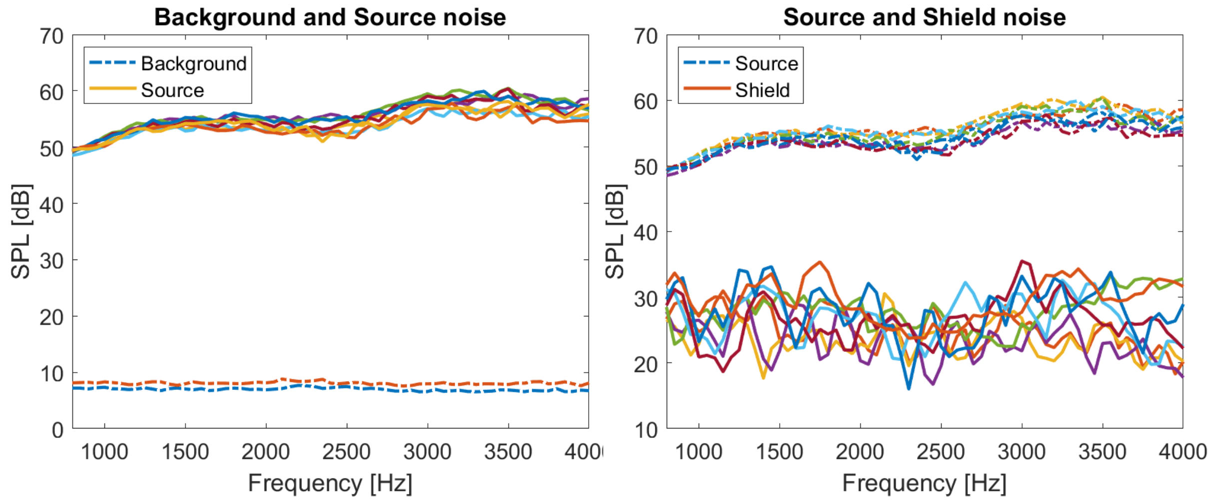

(a) (b)

Figure 4.7: SPL for background, source with and without the shield.

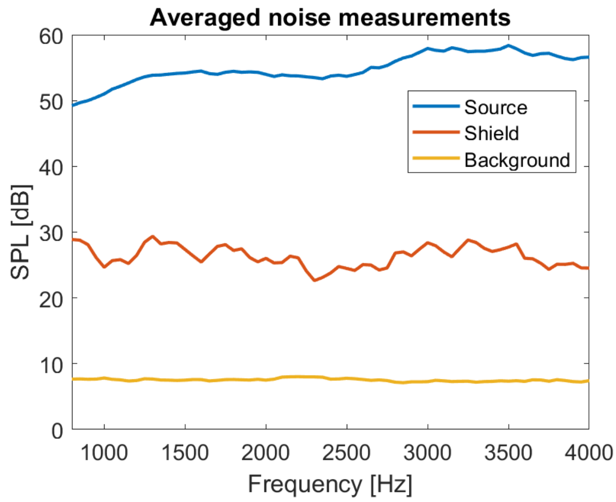

Figure 4.8: Averaged SPL noise measurements, narrow band. This figure depicts the range between each noise, making reference to ISO 3744, each noise should be at least 10 dB apart from each other.

4.4.2 Physical measurements vs Actran simulations

Narrow and 1/3 octave band for TL are shown in fig. 4.9 the Actran values are with the AF01 properties. It was mentioned before that AF01 was an Actran library material since the foam's characterization was not available. Fig. 4.9 shows a close relation with the physical measurements. For this reason a material with similar properties (namely flow resistivity, porosity, etc.) was located in the Volvo Penta's database to get results with a physical and known material for Volvo, this material was introduced in table 3.1 as "MAT 1".

Fig. 4.10 depicts Actran's TL results for each material with the two different propagation models. Fig. 4.10a specifically focuses on the difference between the JCA and Miki models for the AF01 material. At approximately 1600 Hz, the Miki model exhibits a prominent peak in TL. Similarly, this peak is observed for MAT 1 in fig. 4.10b this peak could be due to a resonance effect or the wood component definition in Actran. Fig. 4.10b shows the behaviour for of MAT 1 using both the JCA and Miki models, revealing a similar trend in TL for both models with higher values at high frequencies with the Miki model. In comparison, the AF01 results demonstrate lower TL values for the Miki model.

Finally, fig. 4.11 presents the comparison of TL results obtained from each method with the physical measurements. Figure 4.11a displays the TL results for AF01 and MAT 1 using the JCA model. At higher frequencies, AF01 exhibits a stronger correlation with the physical measurements compared to MAT 1. On the other hand, Figure 4.11b illustrates the TL results for AF01 and MAT 1 utilizing the Miki model. Both materials demonstrate a similar behavior and display a good correlation with the physical measurements within the frequency range of 2000 to 4000 Hz.

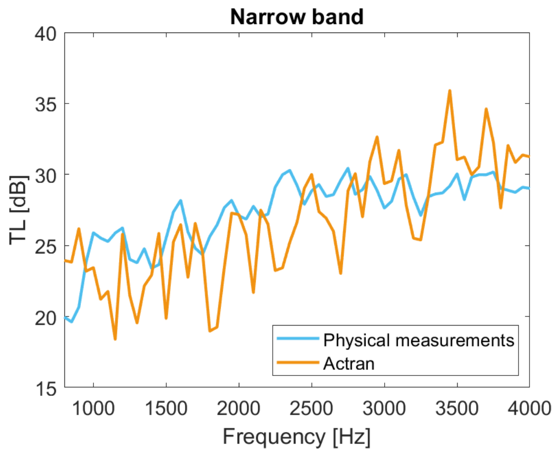

(a) Narrow band (b) 1/3 octave band

Figure 4.9: Transmission loss for narrow and 1/3 octave band for physical measurements and polyurethane foam AF01 for a frequency range of (800 - 4000 Hz).

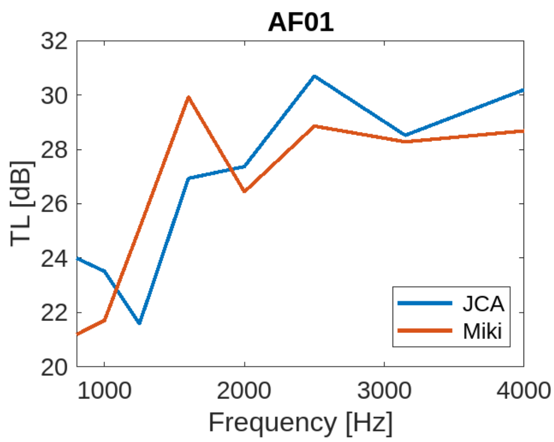

(a) Actran's library material TL results (b) MAT 1 TL results

Figure 4.10: Transmission loss analysis focused on the different materials, AF01 and MAT 1.

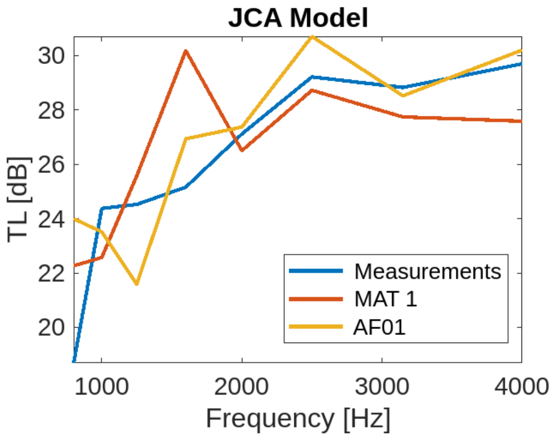

(a) JCA model TL results

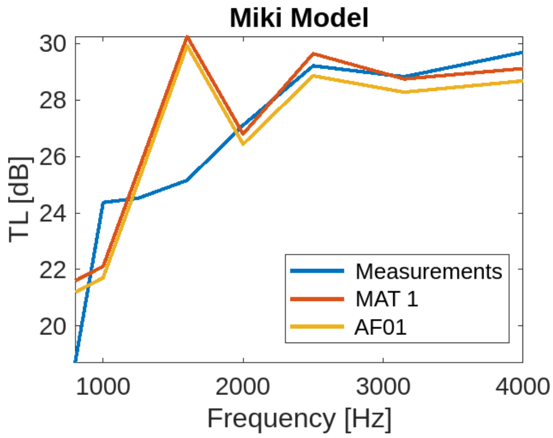

(b) Miki model TL results

Figure 4.11: Transmission loss analysis focused on the different methods, JCA and Miki model.

5

Discussion and Conclusion

5.1 Impedance tube

The impedance tube results highlighted the significant impact of thickness on the behavior of sound propagation in porous materials. Therefore, when physical measurements are available for a specific thickness sample, it is crucial to use that sample in the Actran model. This is because the flow resistivity is dependent on both porosity [17] and thickness, and assuming a linear relationship can lead to incorrect results.

In fig. 3.4, it is evident that manipulating the material parameters has an effect on the sound absorption results. Nonetheless, it is important to note that arbitrarily modifying these parameters in the JCA model may result in a non-existent or difficult-to-manufacture material.

Another important lesson learned is that sound absorption and transmission loss are not directly related, despite their conceptual connection. They are not complementary to each other, and therefore, sound absorption values cannot be directly used for transmission loss analysis.

5.2 Transmission loss

In fig. 4.10a the transmission loss results between the JCA and Miki models exhibit an arbitrary variation between each other for AF01 material. Fig. 4.10b shows a TL behavior with the same tendency but different values at high frequencies. This could be due to the materials properties, since MAT 1 was chosen based on flow resistivity and thickness, disregarding porosity, tortuosity, viscous and thermal length.

Figure 4.11b shows a decrease in TL related to the decrease in flow resistivity. This was expected, the TL behaviour tends to increase with frequency as a consequence of wavelength reduction. A sound wave with a smaller wavelength will allow a greater interaction of the wave with the porous material and more part of the acoustic energy will be transformed into heat. However in fig. 4.6a from the physical measurements a decrease in TL is expected after 5000 Hz.

Regarding the Miki model TL results with flow resistivity variation in fig. 4.10b, a significant spike can be observed at 1600 Hz, indicating an increase of TL approximately of 5 dB with respect to physical measurements. This could be attributed to the wavelength, where the sound wave might have been reflected or an eigenfrequency effect.

It is important to mention a few things from the physical measurements, the velocity-source is composed by a central unit and a nozzle with a tube which was the one inside the shield. However, the central unit made noise, adding noise to the room, for this reason changing the source is recommended in next measurements.

5.3 Conclusion

The initial approximation for transmission loss using Actran simulations exhibited a good first agreement of the transmission loss with respect to the physical measurements. The shield reduced approximately between (20 - 30) dB of the original noise source. Regarding the research questions of this project, the following conclusions were reached:

- **How does the sound parameters affect the sound absorption and transmission loss?**
  The sound absorption in the JCA model can be significantly affected by abrupt changes in sound parameters, as shown in fig. 3.4. Similarly, in transmission loss analysis, the flow resistivity plays a crucial role in modifying the TL results as seen fig. 4.9b with Miki model. Nevertheless due to the characterization of JCA model, modifying randomly the acoustic parameters particularly the tortuosity, viscous and thermal length of the porous material can lead to inaccurate and unreliable results.
- **How does the number of elements per wavelength impact in the final results?**
  For the transmission loss model, a mesh convergence study was not performed due to the complexity and computation time of the model, but the Actran tool for minimum wavelength was used and small elements size were aimed in order to have accurate results. According to the number of elements per wavelength in the solid, porous and finite volume components, the sound wave was well captured in the model. Nevertheless, certain considerations need to be addressed regarding the exterior acoustic mesh. The mesh size in Actran is determined by the exterior acoustic component, which offers different options for mesh design, including near field thickness, adaptive mesh based on frequency, and element type. The current configuration was tested with a maximum of 28 million elements, resulting in excessively long simulation times. Additionally, the number of elements per wavelength remained being 4, for the worst cases, which is below the desired value of 8.
- **How accurate are the simulations in Actran compared to the physical results?**
  Despite the obtained transmission loss results were close to the physical measurements, it is important to highlight the lack of characterization for the wood component, since it is an anisotropic material, therefore improving the accuracy of Actran results should focus on enhancing the acoustic propagation specifically for wood. To assess the accuracy between Actran and physical measurements, the Kundt's tube results can be employed as they solely involve the porous component. The findings indicated good accuracy for the JCA model and a slight over-calculation with the Miki model.

6 Future work

In terms of the ***transmission loss model*** the first step would be to measure the foam material parameters to achieve a final solution for the model. Secondly, improving the exterior acoustic mesh should be a priority to enhance computation time and accuracy in the results. Efforts should be directed towards ANSA to define an appropriate mesh size for the exterior acoustic component. In addition to the mesh improvements, incorporating damping into the structure and conducting a vibro-acoustical analysis would be the next step.

To improve the overall TL of the foam, studies towards compressed foam have been made. Replacing the normal foam for compressed foam in the shield model and study its acoustic behavior would lead to improved results in the overall TL analysis.

For a more realistic source input, a sound radiation field should be defined instead of a spherical source. Furthermore, it would be of interest to compare TL results obtained from an impedance tube model with those from the physical measurements and actual TL model.

For the ***impedance tube*** model, conducting measurements using in-situ equipment, such as an impedance gun, and comparing the obtained impedance values with those from the impedance tube would provide strong validation and establish the model's reliability. Additionally, performing a *layered system analysis* for sound absorption and impedance in the Kundt's tube would be beneficial to ensure accurate results in a wood-foam sample.

Lastly, it is recommended to conduct a reproducibility and repeatability study to ensure the accuracy and reliability of the ***physical measurements***. Although the standard prescribes the use of 10 microphones for these measurements, the technical expert at Volvo Penta approved the use of 8 microphones as sufficiently effective for the test. ISO 3744, Appendix H outlines the details of this study. By implementing this step, the validity and robustness of the physical measurements with 8 microphones can be further confirmed.

Bibliography

[1] Lin, H., Bengisu, T., Mourelatos, Z. P. (2022). “Derivation of acoustic wave equation” in *Lecture notes on acoustics and noise control*, Springer Nature. (pp. 27-48)

[2] Lin, H., Bengisu, T., Mourelatos, Z. P. (2022). “Sound pressure levels and octave bands” in *Lecture notes on acoustics and noise control*, Springer Nature. (pp. 227-251)

[3] MacDonald, S. (2019). “What is A-weighted?”, Retrieved from https://community.sw.siemens.com/s/article/what-is-a-weighting, Siemens DISW.

[4] (2016), “Sound-level meters, A, C and Z frequency weightings for sound”, Retrieved from https://commons.wikimedia.org/wiki/File:Sound-Pressure-Level-Frequency-Weightings-wiki.jpg, Wikipedia commons.

[5] Miles, R. N. (2019). “Sound Transmission Loss” in *Physical approach to engineering acoustics (1st ed.),* Springer Nature. (pp. 53-82)

[6] Ring, T. P., & Langer, S. C. (2022).“On the relationship of the acoustic properties and the microscale geometry of generic porous absorbers”, *Applied Sciences*, 12(21), 11066. Retrieved from https://doi.org/10.3390/app122111066

[7] Carcione, J., (2001), “Biot’s theory for porous media”, in *Handbook of Geophysical Exploration: Seismic Exploration,* Elsevier. (pp. 219–293).

[8] (2018), “Volvo Penta unveils hybrid marine propulsion concept”, Volvo https://www.volvopenta.com/about-us/news-page/2018/jun/volvo-penta-unveils-hybrid-marine-propulsion-concept/

[9] (n.d.), Product data, Retrieved (2023) from https://www.bksv.com/en/transducers /acoustic/acoustic-material-testing-kits/transmission-loss-and-impedance-tube-kits-4206.

[10] Jaouen, L., Gourdon, E., Glé, P. (2020). “Estimation of all six parameters of Johnson-Champoux-Allard-Lafarge model for acoustical porous materials from impedance tube measurements.” *The Journal of the Acoustical Society of America*, 148(4), (pp. 1998-2005). Retrieved from https://doi.org/10.1121/10.0002162

[11] Tao, J., Wang, P., Qiu, X., & Pivity measurements based on the ISO 10534.2 standard impedance tube”, *Building and Environment*, 94, (pp 853–858), retrieved from https://doi.org/10.1016/j.buildenv.2015.06.001

[12] Caballol, D., & Raposo, Á. P., (2018), "Analysis of the measurement of transmission loss in rigid building materials with a standing wave tube" in *Construction and Building Materials*, 182, (pp 242–248), retrieved from https://doi.org/10.1016/j.conbuildmat.2018.06.098

[13] ISO 354:2003. (2018), "Acoustics — Measurement of sound absorption in a reverberation room", *ISO*, retrieved from https://www.iso.org/standard/34545.html

[14] IMO, (n.d.), "Ship noise", Imo.org., Retrieved from https://www.imo.org/en/MediaCentre/HotTopics/Pages/Noise.aspx

[15] WHO. (2001), "Occupational and community noise", *Geneva World Health Organization*, Fact Sheet No. 258. Retrieved from https://www.scielosp.org/article/csp/2006.v22n1/63-68/pt/. [2021-04-25].

[16] Wassilieff, C. (1996). "Sound absorption of wood-based materials". *Applied Acoustics*, 48(4), 339–356. Retrieved from https://doi.org/10.1016/0003-682x(96)00013-8

[17] Lundberg E., (2016). "Micro-structure modelling of acoustics of open porous materials.", *Doctoral dissertation*, KTH.

[18] Takeshi Komatsu, (2008), "Improvement of the Delany-Bazley and Miki models for fibrous sound-absorbing materials", in *Acoust. Sci. & Tech. 29, 2*

[19] Hexagon, (2022) , "Demonstration model - virtual impedance tube", Retrieved from: https://simcompanion.hexagon.com/customers/s/article/Examples-Library-for-Actran

[20] Kaplan M.,Solomon S.,(2016), "A coming boom in commercial shipping? The potential for rapid growth of noise from commercial ships by 2030", Retrieved from: https://www.sciencedirect.com/science/article/abs/pii/S0308597X16303335?via3%Dihub

[21] (n.d), "Abstract Sound Wave Line Background Free Vector", Retrieved from "Vecteezy.com"

[22] Concha-Barrientos M, Campbell-Lendrum D, Steenland K., (2004), "Occupational noise : assessing the burden of disease from work-related hearing impairment at national and local level", *Geneva, World Health Organization*, Environmental Burden of Disease Series, No. 9.

[23] Ginsberg Jerry H., (2021), "Plane waves time domain: solutions" in *Acoustics, a text book for engineers and physicists*, Springer Nature. (pp. 91-183)

[24] Roozen N.B. et al., (2020), “On the experimental characterization of the acoustic properties of Ecophon porous material” in *Forum Acousticum*, Lyon, France. (pp. 01-3108)

[25] Jaouen Luc, (n.d.), “Johnson-Champoux-Allard (JCA) model” in *Acoustical Porous Material Recipes*, Retrieved from: https://apmr.matelys.com/PropagationModels/MotionlessSkeleton/JohnsonChampouxAllardModel.html

[26] Allard J.F., (1993), “Acoustic Impedance at Normal Incidence of Fluids, and Highly Porous Materials” in *Propagation of Sound in Porous Media: Modelling Sound Absorbing Materials*, John Wiley & Sons, Ltd. (pp. 16-30)

DEPARTMENT OF MECHANICS AND MARITIME SCIENCES
CHALMERS UNIVERSITY OF TECHNOLOGY
Gothenburg, Sweden
www.chalmers.se

CHALMERS
UNIVERSITY OF TECHNOLOGY